Inorg. Chem. **2008**, *47*, 2212−2222

Role of Axial Donors in the Ligand Isomerization Processes of Quadruply Bonded Dimolybdenum(II) Compounds†

Moumita Majumdar,‡ Sanjib K. Patra,‡ Mukundamurthy Kannan,‡ Kim R. Dunbar,§ and Jitendra K. Bera*,‡

Department of Chemistry, Indian Institute of Technology, Kanpur 208016, India, and Department of Chemistry, Texas A & M University, College Station, Texas 77843

Received November 22, 2007

Quadruply bonded dimolybdenum(II) complexes with NP-R (2-(2-R)-1,8-naphthyridine; R = thiazolyl (NP-tz), furyl (NP-fu), thienyl (NP-th)) and 2,3-dimethyl-1,8-naphthyridine (NP-Me_2) have been synthesized by reactions of *cis*-$[Mo_2(OAc)_2(CH_3CN)_6][BF_4]_2$ with the corresponding ligands. The products *cis*-$[Mo_2(NP\text{-}tz)_2(OAc)_2][BF_4]_2$ (**1**), *trans*-$[Mo_2(NP\text{-}fu)_2(OAc)_2][BF_4]_2$ (**2**), *trans*-$[Mo_2(NP\text{-}th)_2(OAc)_2][BF_4]_2$ (**3**), and *trans*-$[Mo_2(NP\text{-}Me_2)_2(OAc)_2][BF_4]_2$ (**4**) were isolated and characterized. The NP-R ligands with stronger R = pyridyl and thiazolyl donors result in cis isomers whereas the weaker furyl and thienyl appendages lead to compounds having a trans orientation of the ligands. The use of NP-Me_2 leads to a trans structure with a tetrafluoroborate anion occupying one of the axial sites. Complete replacement of two acetate groups by acetonitrile in **1** and **2** resulted in the cis isomers $[Mo_2(NP\text{-}tz)_2(CH_3CN)_4][OTf]_4$ (**5**) and $[Mo_2(NP\text{-}fu)_2(CH_3CN)_4][OTf]_4$ (**6**) respectively. The combination of one acetate and two acetonitriles as ancillary ligands, however, yields *trans*-$[Mo_2(NP\text{-}tz)_2(OAc)(CH_3CN)_2][BF_4]_3$ (**7**) in the solid state as determined by X-ray crystallography. ^1H NMR spectra of the products are diagnostic of the cis and trans dispositions of the ligands. Solution studies reveal that the ligand arrangements observed in the solid state are mostly retained in the acetonitrile medium. The only exception is **7**, for which a mixture of cis and trans isomers are detected on the NMR time scale. The isolation of trans compounds **2**−**4** from the cis precursor $[Mo_2(OAc)_2(CH_3CN)_6][BF_4]_2$ indicates that an isomerization process occurs during the reactions. The mechanism involving acetate migration through axial coordination has been invoked to rationalize the product formation. Compounds **1**−**7** were structurally characterized by single-crystal X-ray methods.

Introduction

Metal−metal multiply bonded dimetal compounds have proven to be useful for building supramolecular arrays.[1] Initial efforts by Chisholm and co-workers to link M_2 units bridged by carboxylates met with limited success because of facile ligand-scrambling process rendering the formation of both polymers and oligomers.[2] It was later revealed that incorporation of nonlabile bridging ligands into the dimetal core resulted in more directed synthetic targets. Molecular building units of general formula $[M_2^{II}(formamidinate)_{4-n}(CH_3CN)_{2n}]^{n+}$ have been linked by polycarboxylates to generate a variety of molecular architectures including loops, squares, triangles, and polygons.[3] In our research, we have employed the 1,1-bis(diphenylphosphino)methane (dppm) ligand for dirhenium units to build a "dimer of dimers" and molecular triangles.[4] The disposition of the carboxylate groups in the linker and the configuration of the nonlabile ligands in dimetal precursors dictate the resulting topology of the molecular architecture. For a linear dicarboxylate linker, *cis*-$M_2(formamidinate)_2$ corners lead to a discrete

* To whom correspondence should be addressed. E-mail: jbera@iitk.ac.in.

† Dedicated to the memory of Professor F. A. Cotton.

‡ Indian Institute of Technology.

§ Texas A & M University.

(1) (a) Chisholm, M. H.; Macintosh, A. M. *Chem. Rev.* **2005**, *105*(8), 2949. (b) Cotton, F. A.; Lin, C.; Murillo, C. A. *Proc. Natl. Acad. Sci. U.S.A.* **2002**, *99*, 4810. (c) Cotton, F. A.; Lin, C.; Murillo, C. A. *Acc. Chem. Res.* **2001**, *34*, 759. (d) Chisholm, M. H. *Acc. Chem. Res.* **2000**, *33*, 53.

(2) (a) Chisholm, M. H.; Cotton, F. A.; Daniels, L. M.; Folting, K.; Huffman, J. C.; Iyer, S. S.; Lin, C.; Maclntosh, A. M.; Murillo, C. A. *J. Chem. Soc., Dalton Trans.* **1999**, 1387. (b) Cayton, R. H.; Chisholm, M. H.; Huffman, J. C.; Lobkovsky, E. B. *Angew. Chem., Int. Ed.* **1991**, *30*, 862. (c) Cayton, R. H.; Chisholm, M. H.; Huffman, J. C.; Lobkovsky, E. B. *J. Am. Chem. Soc.* **1991**, *113*, 8709.

10.1021/ic702298v CCC: $40.75
Published on Web 02/12/2008

Scheme 1

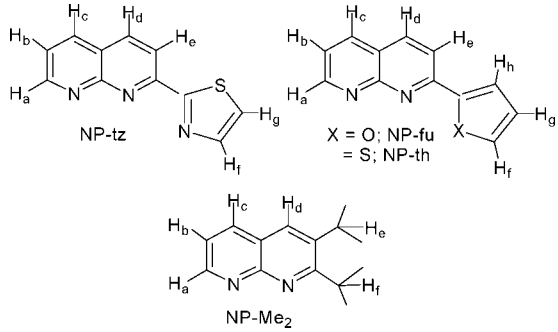

Scheme 2

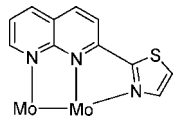

cyclic structure whereas a ladder structure is favored for its trans congener.[1,2] Directed synthesis of a particular stereoisomer of the dimetal core is essential for constructing molecular architectures of desired topologies.

Our interest involves the chemistry of neutral tridentate ligands of the type NP-R (2-(2-R)-1,8-naphthyridine; R = thiazolyl, furyl, thienyl) and 2,3-dimethyl-1,8-naphthyridine.[5] The assortment of ligands employed in this work along with their nomenclature is shown in Scheme 1. The N-C-N moiety bridges the dimetal core and the appendage at the 2-position of NP core binds to the axial position of the dimetal core as illustrated for NP-tz in Scheme 2.[6]

Earlier studies involving 2-(2-pyridyl)-1,8-naphthyridine (NP-py) with metal-metal bonded dimetal complexes led to exclusively cis products as in the case of the $[M_2^{II}(OAc)_2(NP\text{-}py)_2]^{2+}$ (M = Mo, Rh, Ru)[7] compounds. Herein we report the syntheses of quadruply bonded dimolybdenum(II) complexes with two nonlabile NP-R ligands with the remaining equatorial sites occupied by acetate and/or acetonitrile ligands. The cis and trans products of general formula $[Mo_2(NP\text{-}R)_2(OAc)_{2-n}(CH_3CN)_{2n}]^{n+2}$ ($n = 0, 1, 2$), obtained from *cis*-$[Mo_2(OAc)_2(CH_3CN)_6]^{2+}$, underscore the importance of the axial appendage in the ligand-isomerization process. The reactivity of the compounds and the ligand configuration in the final products are rationalized on the basis of the hierarchy of ligand labilities and the thermodynamic stabilities of the compounds.

Experimental Section

General Procedure. Materials. All manipulations were carried out under an inert atmosphere with the use of standard Schlenk-line techniques. Glassware was flame-dried under a vacuum prior to use. Solvents were dried by conventional methods, distilled over nitrogen and deoxygenated prior to use.[8] The reagents $Mo(CO)_6$, HBF_4 (51–57% in diethyl ether), and Et_3OBF_4 (1 M in CH_2Cl_2) were purchased from Aldrich. Trifluoromethane sulfonic acid was purchased from Spectrochem, India. The starting materials $[Mo_2(OAc)_4]$,[9] *cis*-$[Mo_2(OAc)_2(CH_3CN)_6][BF_4]_2$,[10] and $[Mo_2(CH_3CN)_{10}][BF_4]_4$[11] were synthesized according to the literature procedures. $[Mo_2(CH_3CN)_{10}][OTf]_4$[12] was prepared by a modified synthetic procedure using $[Mo_2(OAc)_4]$ and trifluoromethane sulfonic acid at room temperature for 1 h. The ligands 2-(2-pyridyl)-1,8-Naphthyridine (NP-py), 2-(2-thiazolyl)-1,8-naphthyridine (NP-tz), 2-(2-furyl)-1,8-naphthyridine (NP-fu), 2-(2-thienyl)-1,8-naphthyridine (NP-th), and 2,3-dimethyl-1,8-naphthyridine (NP-Me_2) were prepared by the Friedlander condensation of 2-aminonicotinaldehyde with corresponding acyl derivatives.[13] Synthetic procedures and NMR data for the ligands are provided as Supporting Information.

Physical Measurements. Infrared spectra were recorded in the range 4000–400 cm^{-1} on a Vertex 70 Bruker spectrophotometer on KBr pellets. ^1H NMR spectra were obtained on a JEOL JNM-LA 400 MHz spectrometer. Electronic absorptions were measured on a Lambda-20 Perkin-Elmer spectrophotometer. Cyclic voltam-

(3) (a) Cotton, F. A.; Murillo, C. A.; Zhao, Q. *Inorg. Chem.* **2007**, *46*, 6858. (b) Cotton, F. A.; Jin, J. Y.; Li, Z.; Liu, C. Y.; Murillo, C. A. *Dalton Trans.* **2007**, 2328. (c) Cotton, F. A.; Li, Z.; Liu, C. Y.; Murillo, C. A.; Zhao, Q. *Inorg. Chem.* **2006**, *45*, 6387. (d) Cotton, F. A.; Liu, C. Y.; Murillo, C. A.; Zhao, Q. *Inorg. Chem.* **2006**, *45*, 9493. (e) Cotton, F. A.; Li, Z.; Liu, C. Y.; Murillo, C. A.; Zhao, Q. *Inorg. Chem.* **2006**, *45*, 9480. (f) Cotton, F. A.; Li, Z.; Liu, C. Y.; Murillo, C. A.; Wang, X. *Inorg. Chem.* **2006**, *45*, 2619. (g) Cotton, F. A.; Murillo, C. A.; Yu, R. *Inorg. Chim. Acta* **2006**, *359*, 4811. (h) Cotton, F. A.; Murillo, C. A.; Yu, R. *Dalton Trans.* **2006**, 3900. (i) Cotton, F. A.; Donahue, J. P.; Murillo, C. A.; Yu, R. *Inorg. Chim. Acta* **2005**, *358*, 1373. (j) Cotton, F. A.; Li, Z.; Liu, C. Y.; Murillo, C. A.; Wang, X. *Chem. Commun.* **2003**, 2190. (k) Berry, J. F.; Cotton, F. A.; Ibragimov, S. A.; Murillo, C. A.; Wang, X. *Dalton Trans.* **2003**, 4297. (l) Cotton, F. A.; Daniels, L. M.; Lin, C.; Murillo, C. A. *J. Am. Chem. Soc.* **1999**, *121*, 4538.

(4) (a) Bera, J. K.; Basca, J.; Smucker, B. W.; Dunbar, K. R. *Eur. J. Inorg. Chem.* **2004**, 368. (b) Bera, J. K.; Clerac, R.; Fanwick, P. E.; Walton, R. A. *J. Chem. Soc., Dalton Trans.* **2002**, 2168. (c) Bera, J. K.; Smucker, B. W.; Walton, R. A.; Dunbar, K. R. *Chem. Commun.* **2001**, 2562. (d) Bera, J. K.; Angaridis, P.; Cotton, F. A.; Petrukhina, M. A.; Fanwick, P. E.; Walton, R. A. *J. Am. Chem. Soc.* **2001**, *123*, 1515.

(5) (a) Patra, S. K.; Bera, J. K. *Organometallics* **2006**, 6054. (b) Patra, S. K.; Majumdar, M.; Bera, J. K. *J. Organomet. Chem.* **2006**, *691*, 4779. (c) Patra, S. K.; Sadhukhan, N.; Bera, J. K. *Inorg. Chem.* **2006**, *45*, 4007.

(6) (a) Collin, J.-P.; Jouaiti, A.; Sauvage, J.-P.; Kaska, W. C.; McLoughlin, M. A.; Keder, N. L.; Harrison, W. T. A.; Stucky, G. D. *Inorg. Chem.* **1990**, *29*, 2238. (b) Binamira-Soriaga, E.; Keder, N. L.; Kaska, W. C. *Inorg. Chem.* **1990**, *29*, 3167. (c) Thummel, R. P.; Decloitre, Y. *Inorg. Chim. Acta* **1987**, *128*, 245. (d) Binamira-Soriaga, E.; Sprouse, S. D.; Watts, R. J.; Kaska, W. C. *Inorg. Chim. Acta* **1984**, *84*, 135. (e) Tikkanen, W. R.; Krüger, C.; Bomben, K. D.; Jolly, W. L.; Kaska, W, C.; Ford, P. C. *Inorg. Chem.* **1984**, *23*, 3633. (f) Baker, A. T.; Tikkanen, W. R.; Kaska, W. C.; Ford, P. C. *Inorg. Chem.* **1984**, *23*, 3254. (g) Tikkanen, W.; Binamira-Soriaga, E.; Kaska, W.; Ford, P. *Inorg. Chem.* **1983**, *22*, 1147. (h) Caluwe, P.; Evens, G. *Macromolecules* **1979**, *12*, 803.

(7) (a) Campos-Fernandez, C. S.; Thomson, L. M.; Galan-Mascaros, J. R.; Ouyang, X.; Dunbar, K. R. *Inorg. Chem.* **2002**, *41*, 1523. (b) Campos-Fernandez, C. S.; Ouyang, X.; Dunbar, K. R. *Inorg. Chem.* **2000**, *39*, 2432.

(8) Perrin, D. D.; Armarego, W. L. F.; Perrin, D. R. *Purification of Laboratory Chemicals*, 2nd ed.; Pergamon Press: New York, 1980.

(9) (a) Cotton, F. A.; Mester, Z. C.; Webb, T. R. *Acta Crystallogr., Sect. B* **1974**, *30*, 2768. (b) Brignole, A. B.; Coton, F. A. *Inorg. Synth.* **1972**, *13*, 87. (c) Lawton, D.; Mason, R. *J. Am. Chem. Soc.* **1965**, *87*, 921.

(10) (a) Clegg, W.; Pimblett, G.; Garner, C. D. *Polyhedron* **1986**, *5*, 31. (b) Pimblett, G.; Garner, C. D.; Clegg, W. *J. Chem. Soc., Dalton Trans.* **1986**, 1257. (c) Cotton, F. A.; Reid, A. H.; Schwotzer, W. *Inorg. Chem.* **1985**, *24*, 3965.

(11) (a) Cotton, F. A.; Wieinger, K. J. *Inorg. Synth.* **1992**, *29*, 134. (b) Cotton, F. A.; Eglin, J. L.; Wiesinger, K. J. *Inorg. Chim. Acta* **1992**, *195*, 11. (c) Cotton, F. A.; Wiesinger, K. J. *Inorg. Chem.* **1991**, *30*, 871. (d) Telser, J.; Drago, R. S. *Inorg. Chem.* **1984**, *23*, 1798.

(12) Mayer, J. M.; Abbott, E. H. *Inorg. Chem.* **1983**, *22*, 2774.

(13) (a) Reddy, K. V.; Mogilaiah, K.; Sreenivasulu, B. *J. Ind. Chem. Soc.* **1986**, *63*, 443. (b) Thummel, R. P.; Lefoulon, F.; Cantu, D.; Mahadevan, R. J. *J. Org. Chem.* **1984**, *49*, 2208. (c) Majewicz, T. C.; Caluwe, P. *J. Org. Chem.* **1974**, *39*, 720. (d) Hawes, E. M.; Wibberley, D. G. *J. Chem. Soc.* **1966**, 315.

metric studies were performed on a BAS Epsilon electrochemical workstation in acetonitrile with 0.1 M tetra-*n*-butylammonium hexafluorophosphate ($TBAPF_6$) as the supporting electrolyte. The working electrode was a BAS Pt disk electrode, the reference electrode was Ag/AgCl, and the auxiliary electrode was a Pt wire. The ferrocene/ferrocenium couple occurs at $E_{1/2} = +0.51$ (70) V versus Ag/AgCl under the same experimental conditions. The potentials are reported in volts (V); the ΔE ($E_{p,a} - E_{p,c}$) values are in millivolts (mV) at a scan rate of 100 mVs^{-1}.

X-ray Data Collection and Refinement. Single-crystal X-ray studies were performed on a CCD Bruker SMART APEX diffractometer equipped with an Oxford Instruments low-temperature attachment. Data for **1** was collected at room temperature (18 °C), whereas others were collected at 100(2) K using graphite-monochromated Mo Kα radiation ($\lambda_\alpha = 0.71073$ Å). The frames were integrated in the Bruker SAINT software package,[14] and the data were corrected for Lorentz and polarization effects. An absorption correction was applied.[15] Structures were solved and refined with the SHELX suite of programs[16] as implemented in X-seed.[17] An empirical absorption correction was applied for compound **4** using XABS2.[18] Hydrogen atoms of the ligands, unless mentioned otherwise, were included in the final stages of the refinement and were refined with a typical riding model. ORTEP-III was used to produce the diagrams.[19] Pertinent crystallographic data for compounds **1–7** are summarized in Table 1. Structure solution and refinement details for compounds **1**−**7** are provided in the Supporting Information.

Synthesis of *cis*-$[Mo_2(NP\text{-}tz)_2(OAc)_2]$ $[BF_4]_2$ (1). A sample of $[Mo_2(OAc)_2(CH_3CN)_6][BF_4]_2$ (71 mg, 0.10 mmol) dissolved in 20 mL of CH_3CN was treated with NP-tz (46 mg, 0.22 mmol), which led to a color change from light pink to dark green. After 8 h of stirring at room temperature, the solution was concentrated under a vacuum and 15 mL of toluene was added with stirring to induce precipitation. The resulting solid residue was washed with toluene (2 × 10 mL) and 10 mL of diethyl ether; dried in vacuum. Yield: 76 mg (86%). ^{1}H NMR (CD_3CN, δ): 8.98 (d, 1H); 8.81 (dd, 1H); 8.57 (d, 1H); 8.01 (d, 1H); 7.83 (dd, 1H); 7.78 (q, 1H); 7.48 (d, 1H); 2.67 (s, 3H). IR (KBr, cm^{-1}): ν(OAc^-): 1604, 1438; ν(BF_4^-) 1087. UV–vis data (λ_{max}, nm (log ϵ)): 271 (4.12), 450 (3.14), 656 (2.40), 877 (2.73). Anal. Calcd for $C_{26}H_{20}N_6S_2O_4B_2F_8Mo_2$: C, 34.31; H, 2.22; N, 9.23. Found: C, 34.50; H, 2.32; N, 9.46.

Synthesis of *trans*-$[Mo_2(NP\text{-}fu)_2(OAc)_2][BF_4]_2$ (2). The reaction of $[Mo_2(OAc)_2(CH_3CN)_6][BF_4]_2$ (59 mg, 0.08 mmol) and NP-fu (37 mg, 0.19 mmol) was carried out following a procedure similar to that described for the synthesis of complex **1**. The solution color underwent an instantaneous color change from light pink to bright green upon addition of NP-fu. The solid residue obtained was washed with toluene (2 × 10 mL) and 10 mL of diethyl ether and dried in vacuum. Yield: 60 mg (85%). ^{1}H NMR (CD_3CN, δ): 8.96 (m, 2H); 8.53 (q, 1H); 8.46 (d, 1H); 8.10 (q, 1H); 7.86 (d, 1H); 7.49 (s, 1H); 6.84 (m, 1H); 2.53 (s, 3H). IR (KBr, cm^{-1}): ν(OAc^-): 1611, 1442; ν(BF_4^-) 1069. UV–vis data (λ_{max}, nm (log ϵ)): 273

Table 1. Crystallographic Data and Refinement Parameters for **1–7**

	1·0.5 CH_3CN	**2**	**3**·2 CH_3CN	**4**	**5**·CH_3CN	**6**	**7**·C_6H_6
empirical formula	$C_{27}H_{20}B_2F_8Mo_2N_{6.5}O_4S_2$	$C_{28}H_{22}B_2F_8Mo_2N_4O_6$	$C_{32}H_{28}B_2F_8Mo_2N_6O_4S_2$	$C_{24}H_{26}B_2F_8Mo_2N_4O_4$	$C_{36}H_{29}F_{12}Mo_2N_{11}O_{12}S_6$	$C_{35}H_{16}BF_{13}Mo_2N_8O_{11}S_3$	$C_{34}H_{29}B_3F_{12}Mo_2N_6O_2S_2$
fw	929.11	876.00	990.22	799.99	1419.94	1270.43	1098.08
cryst syst	monoclinic	monoclinic	triclinic	monoclinic	triclinic	monoclinic	monoclinic
space group	*C*2/*c*	$P2_1/n$	$P\bar{1}$	*Pc*	$P\bar{1}$	*C*2/*c*	*C*2/*c*
a (Å)	31.955(12)	9.7031(19)	11.402(3)	8.8716(9)	11.4556(12)	36.337(3)	36.9728(19)
b (Å)	15.125(5)	13.741(3)	17.573(5)	14.1930(14)	13.1497(14)	11.5014(9)	16.4436(8)
c (Å)	15.023(4)	11.596(2)	19.138(6)	12.5880(9)	19.465(2)	20.6550(18)	14.5941(7)
α (deg)	90.00	90.00	60.427(4)	90.00	77.161(2)	90.00	90.00
β (deg)	113.755(9)	101.12(3)	65.638(4)	117.177(5)	73.071(2)	128.738(3)	112.4510(10)
γ (deg)	90.00	90.00	79.305(4)	90.00	69.556(2)	90.00	90.00
V (Å^3)	6646(4)	1517.2(5)	3037.3(16)	1410.0(2)	2604.6(5)	4880.4(7)	8200.2(7)
Z	8	2	3	2	2	4	8
ρ_{calcd} (g cm^{-3})	1.857	1.918	1.624	1.884	1.811	1.729	1.779
no. of reflns collected	22017	9885	8626	9208	14957	12131	26927
no. of independent reflns	8197	3721	8626	4711	10355	4120	10013
no. of reflns obsd [$I > 2\ \sigma(I)$]	6346	3168	5189	4515	8632	3423	8013
GOF	1.035	1.049	1.011	1.074	1.104	1.380	1.055
final R indices [$I > 2\sigma(I)$], R1[a]	0.0523	0.0490	0.0983	0.0583	0.0954	0.1075	0.0508
final R indices [$I > 2\sigma(I)$], wR2[a]	0.1253	0.1115	0.2218	0.1415	0.2175	0.3118	0.1070
R indices (all data), R1[a]	0.0707	0.0591	0.1529	0.0606	0.1109	0.1196	0.0731
R indices (all data), wR2[a]	0.1351	0.1165	0.2501	0.1435	0.2277	0.3264	0.1178

[a] $R_1 = \Sigma||F_o| - |F_c||/\Sigma|F_o|$ with $F_o^2 > 2\sigma(F_o^2)$. $wR_2 = [\Sigma w(|F_o^2| - |F_c^2|)^2/\Sigma|F_o^2|^2]^{1/2}$.

(14) *SAINT+ Software for CCD Diffractometers*; Bruker AXS: Madison, WI 2000.

(15) Sheldrick, G. M. *SADABS Program for Correction of Area Detector Data*; University of Göttingen: Göttingen, Germany, 1999.

(16) (a) *SHELXTL Package*,version 6.10; Bruker AXS: Madison, WI, 2000. (b) Sheldrick, G. M. *SHELXS-86 and SHELXL-97*; University of Göttingen: Göttingen, Germany, 1997.

(17) (a) Atwood, J. L.; Barbour, L. J. *Cryst. Growth Des.* **2003**, *3*, 3. (b) Barbour, L. J. *J. Supramol. Chem.* **2001**, *1*, 189.

(18) Parkin, S. R.; Moezzi, B.; Hope, H. *J. Appl. Crystallogr.* **1995**, *28*, 53.

(19) Farrugia, L. J. *J. Appl. Crystallogr.* **1997**, *30*, 565.

(4.79), 382 (4.70), 693 (2.94). Anal. Calcd for $C_{28}H_{22}N_4O_6B_2F_8Mo_2$: C, 38.39; H, 2.53; N, 6.39. Found: C, 38.54; H, 2.71; N, 6.58.

Synthesis of *trans*-[Mo$_2$(NP-th)$_2$(OAc)$_2$][BF$_4$]$_2$ (3). The reaction of $[Mo_2(OAc)_2(CH_3CN)_6][BF_4]_2$ (50 mg, 0.07 mmol) and NP-th (32 mg, 0.15 mmol) was carried out following a similar procedure described for the synthesis of complex **1**. A dramatic color change occurred from pink to green upon ligand addition. The solid was washed with toluene (2 × 10 mL) and 10 mL of diethyl ether and dried in vacuum. Yield: 52 mg (83%). IR (KBr, cm^{-1}): ν(OAc$^-$): 1615, 1440; ν(BF$_4^-$) 1072. UV–vis data (λ_{max}, nm (log ϵ)): 280 (4.68), 380 (4.50), 676 (2.71). Anal. Calcd for $C_{28}H_{22}N_4O_4S_2B_2F_8Mo_2$: C, 37.03; H, 2.44; N, 6.17. Found: C, 37.15; H, 2.59; N, 6. 25.

Synthesis of *trans*-[Mo$_2$(NP-Me$_2$)$_2$(OAc)$_2$][BF$_4$]$_2$ (4). The reaction of $[Mo_2(OAc)_2(CH_3CN)_6][BF_4]_2$ (63 mg, 0.09 mmol) and NP-Me$_2$ (38 mg, 0.23 mmol) was carried out following a similar procedure described for the synthesis of complex **1**. The resulting green colored solution was concentrated under a vacuum, and 15 mL of diethyl ether was added with stirring to induce precipitation. The solid residue was washed with diethyl ether (3 × 10 mL) and dried in vacuum. Yield: 58 mg (84%). ^{1}H NMR (CD_3CN, δ): 8.88 (m, 2H); 8.73 (s, 1H); 8.05 (q, 1H); 2.57 (s, 3H); 2.59 (s, 3H); 1.79 (s, 3H). IR (KBr, cm^{-1}): ν(OAc$^-$): 1614, 1444; ν(BF$_4^-$) 1064. UV–vis data (λ_{max}, nm (log ϵ)): 288 (4.48), 319 (4.45), 628 (2.73). Anal. Calcd for $C_{24}H_{26}N_4O_4B_2F_8Mo_2$: C, 36.03; H, 3.28; N, 7.00. Found: C, 36.12; H, 3.36; N, 7.11.

Synthesis of *cis*-[Mo$_2$(NP-tz)$_2$(CH$_3$CN)$_4$][OTf]$_4$ (5). Method A: An acetonitrile solution (10 mL) of NP-tz (31 mg, 0.14 mmol) was added dropwise to an acetonitrile solution (15 mL) of $[Mo_2(CH_3CN)_{10}][OTf]_4$, and the solution was stirred for 8 h at room temperature. The resulting green-colored solution was concentrated under a vacuum, and 15 mL of toluene was added with stirring to induce precipitation. The resulting solid was washed with toluene (2 × 10 mL) and 10 mL of diethyl ether; dried in a vacuum. Yield: 68 mg (85%). ^{1}H NMR (CD_3CN, δ): 9.23 (d, 1H); 9.06 (d, 1H); 8.69 (d, 1H); 8.06 (d, 1H); 7.93 (q, 1H); 7.73 (dd, 1H); 7.38 (d, 1H). IR (KBr, cm^{-1}): ν(CN) 2922; ν(OTf$^-$) 1262. UV–vis data (λ_{max}, nm (log ϵ)): 269 (4.81), 332 (4.65), 401 (4.71), 747 (3.25). Anal. Calcd for $C_{34}H_{26}N_{10}O_{12}S_6F_{12}Mo_2$: C, 29.62; H, 1.90; N, 10.16. Found: C, 29.81; H, 2.03; N, 10.29.

Method B: To an acetonitrile solution (20 mL) of *cis*-$[Mo_2(NP\text{-}tz)_2(OAc)_2][BF_4]_2$ (71 mg, 0.08 mmol) was added triflic acid (0.02 mL, 0.16 mmol) dropwise with stirring. The solution was stirred at room temperature for 1 h, the solution was concentrated under a vacuum, and 15 mL of diethyl ether was added with stirring to induce precipitation. The solid residue obtained was washed with diethyl ether (3 × 10 mL) and dried in a vacuum. Yield: 90 mg (84%).

Synthesis of *cis*-[Mo$_2$(NP-fu)$_2$(CH$_3$CN)$_4$][OTf]$_4$ (6). Method A: To an acetonitrile solution (20 mL) of *trans*-$[Mo_2(NP\text{-}fu)_2(OAc)_2][BF_4]_2$ (55 mg, 0.06 mmol) was added triflic acid (0.01 mL, 0.13 mmol) dropwise with stirring. The initial green solution, which turned a bright hue, was stirred at room temperature for 1 h. The resulting bright-green-colored solution was concentrated under a vacuum, and 15 mL of diethyl ether was added with stirring to induce precipitation of a solid that was washed with diethyl ether (3 × 10 mL) and dried in vacuum. Yield: 73 mg (86%). ^{1}H NMR (CD_3CN, δ): 9.01 (d, 1H); 8.97 (m, 1H); 8.47 (d, 1H); 7.97 (m, 1H); 7.92 (d, 1H); 7.83 (dd, 1H); 7.39 (d, 1H); 6.87 (m, 1H). IR (KBr, cm^{-1}): ν(CN) 2922; ν(OTf$^-$) 1268; ν(BF$_4^-$) 1028. UV–vis data (λ_{max}, nm (log ϵ)): 272 (4.45), 354 (4.01), 398 (4.26), 765 (2.58). Anal. Calcd for $C_{36}H_{28}N_8O_{14}S_4F_{12}Mo_2$: C, 32.15; H, 2.09; N, 8.33. Found: C, 32.28; H, 2.17; N, 8.52.

Method B: An acetonitrile solution (10 mL) of NP-fu (35 mg, 0.18 mmol) was added dropwise to an acetonitrile solution (15 mL) of $[Mo_2(CH_3CN)_{10}][BF_4]_4$ (0.07 mg, 0.08 mmol) and the solution was stirred for 8 h at room temperature. The resulting bright-green-colored solution was concentrated under a vacuum, and 15 mL of toluene was added with stirring to induce precipitation. The solid residue obtained was washed with toluene (2 × 10 mL) and 10 mL of diethyl ether; dried in vacuum. The compound was crystallized by layering the acetonitrile solution over toluene, using [*n*-Bu$_4$N][OTf] for anion exchange. Yield: 62 mg (87%).

Synthesis of *trans*-[Mo$_2$(NP-tz)$_2$(OAc)(CH$_3$CN)$_2$][BF$_4$]$_3$ (7). To an acetonitrile solution (15 mL) of *cis*-$[Mo_2(NP\text{-}tz)_2(CH_3CN)_4][BF_4]_4$ (51 mg, 0.05 mmol) were added acetonitrile solutions (10 mL) of [n-Bu$_4$N][OAc] (19 mg, 0.06 mmol) dropwise and the solution was stirred for 8 h at room temperature. The resulting green-colored solution was concentrated under a vacuum, and 15 mL of toluene was added with stirring to induce precipitation. The solid was washed with toluene (2 × 10 mL) and 10 mL of diethyl ether and dried in a vacuum. Yield: 38 mg (82%).^{1}H NMR (CD_3CN, δ): 9.31 (d); 9.23 (q); 9.13 (m); 8.79 (d); 8.74 (m); 8.59 (m); 8.31 (q); 8.23 (m); 8.01 (d); 7.98 (q); 7.49 (d); 7.47 (d); 2.50 (s) and 2.43 (s). IR (KBr, cm^{-1}): ν(CN): 2922; ν(OAc$^-$): 1606, 1439; ν(BF$_4^-$) 1060. UV–vis data (λ_{max}, nm (log ϵ)): 273 (4.13), 306 (4.04), 375 (4.23). Anal. Calcd for $C_{28}H_{23}N_8O_2S_2B_3F_{12}Mo_2$: C, 32.97; H, 2.27; N, 10.99. Found: C, 33.10; H, 2.39; N, 11.07.

Conversion of *cis*-[Mo$_2$(NP-tz)$_2$(CH$_3$CN)$_4$]$^{4+}$ to *cis*-[Mo$_2$(NP-tz)$_2$(OAc)$_2$]$^{2+}$. An acetonitrile solution (15 mL) of *cis*-$[Mo_2(NP\text{-}tz)_2(CH_3CN)_4][BF_4]_4$ (58 mg, 0.05 mmol) was treated with an acetonitrile solution (10 mL) of [*n*-Bu$_4$N][OAc] (34 mg, 0.01 mmol) by dropwise addition and the solution was stirred for 8 h at room temperature. The resulting green-colored solution was concentrated under vacuum, and 15 mL of toluene was added with stirring to induce precipitation. The solid residue was washed with toluene (2 × 10 mL) and 10 mL of diethyl ether and dried in a vacuum. Yield: 40 mg (85%). The ^{1}H NMR spectrum of the isolated product is identical to that of **1**. The identity of the product was further confirmed by examining the cell parameters by single crystal X-ray diffraction.

Conversion of *cis*-[Mo$_2$(NP-fu)$_2$(CH$_3$CN)$_4$]$^{4+}$ to *trans*-[Mo$_2$(NP-fu)$_2$(OAc)$_2$]$^{2+}$. The reaction of *cis*-$[Mo_2(NP\text{-}fu)_2(CH_3CN)_4][BF_4]_4$ (56 mg, 0.06 mmol) and [*n*-Bu$_4$N][OAc] (0.04 mg, 0.13 mmol) in acetonitrile was carried out following a similar procedure as described in the aforementioned reaction. The solid residue was washed with toluene (2 × 10 mL) and 10 mL diethyl ether and dried in a vacuum. Yield: 81 mg (85%). The product was identified as being **2** from the ^{1}H NMR spectrum and cell parameters.

Conversion of 7 to 1. The reaction of an acetonitrile solution of complex **7** (29 mg, 0.03 mmol) and [*n*-Bu$_4$N][OAc] (14 mg, 0.05 mmol) was carried out following a similar procedure as described above. The solid residue was washed with toluene (2 × 10 mL) and 10 mL of diethyl ether and dried in a vacuum. Yield: 23 mg (86%). Compound **1** was identified by ^{1}H NMR and X-ray data.

Results and Discussion

Synthesis. The syntheses of compounds **1**−**7** are schematically represented in Schemes 3 and 4. The notation in bold below each arrowhead refers to the individual transformations. Reaction of *cis*-$[Mo_2(OAc)_2(CH_3CN)_6][BF_4]_2$ with 2-(2-thiazolyl)-1,8-naphthyridine (NP-tz) in acetonitrile readily forms *cis*-$[Mo_2(NP\text{-}tz)_2(OAc)_2][BF_4]_2$ (**1**) (**3a**). An analogous compound *cis*-$[Mo_2(NP\text{-}py)_2(OAc)_2][BF_4]_2$ was

Scheme 3

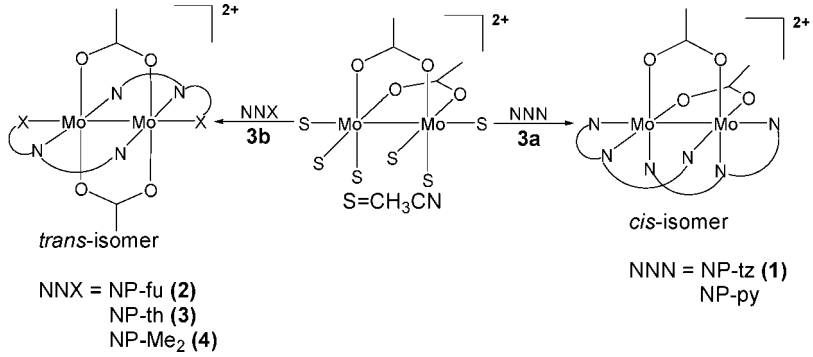

Scheme 4

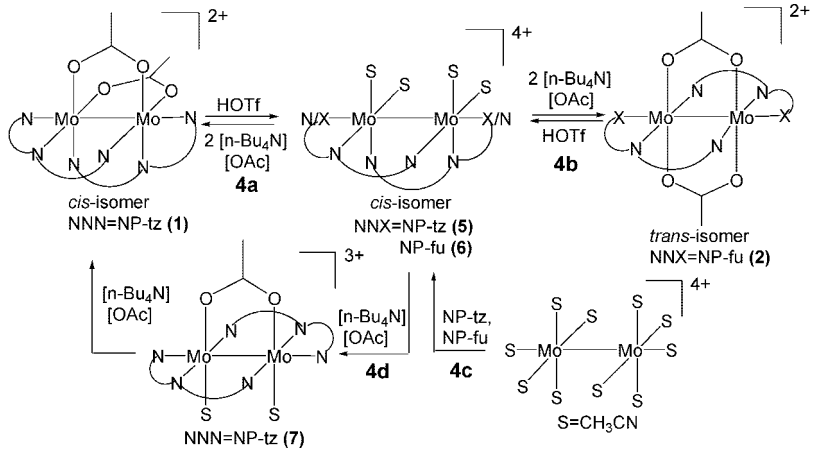

reported earlier from a similar reaction with 2-(2-pyridyl)-1,8-naphthyridine (NP-py).[7] Compound **1** was also obtained from the reaction of $Mo_2(OAc)_4$ with NP-tz in the presence of an excess of 2 equiv of [n-Bu_4N][BF_4]. On the contrary, trans products result from the reactions of *cis*-[$Mo_2(OAc)_2(CH_3CN)_6$][BF_4]$_2$ with 2-(2-furyl)-1,8-naphthyridine (NP-fu), 2-(2-thienyl)-1,8-Naphthyridine (NP-th) and 2,3-dimethyl-1,8-naphthyridine (NP-Me_2). The isolated products are *trans*-[Mo_2(NP-fu)$_2(OAc)_2$][BF_4]$_2$ (**2**), *trans*-[Mo_2(NP-th)$_2(OAc)_2$]-[BF_4]$_2$ (**3**) and *trans*-[Mo_2(NP-Me_2)$_2(OAc)_2$][BF_4]$_2$ (**4**), respectively (**3b**). The identities of isomers are assigned solely on the basis of their solid-state structures. Notably, only the trans isomer was isolated from the reaction of $Mo_2(OAc)_4$ and DAniFH (*N*,*N*′-di-*p*-anisyl formamidine).[20]

Protonation of **1** with triflic acid in acetonitrile leads to the replacement of bridging acetate groups by acetonitrile ligands to yield *cis*-[Mo_2(NP-tz)$_2(CH_3CN)_4$][OTf]$_4$ (**5**). The reagents $HBF_4 \cdot Et_2O$ and Me_3OBF_4 produce identical tetracationic species [Mo_2(NP-tz)$_2(CH_3CN)_4$]$^{4+}$,[4a] but single crystals suitable for X-ray studies were obtained only with triflates as the counterions (**4a**). Treatment of triflic acid with **2** readily produces *cis*-[Mo_2(NP-fu)$_2(CH_3CN)_4$][OTf]$_4$ (**6**). It is noted that the configuration of NP-fu ligands in the precursor molecule **2** is trans, whereas the ligands are cis to each other in compound **6** (**4b**).

An alternate route to the cis compounds **5** and **6** is the reaction of NP-tz and NP-fu, respectively, with [$Mo_2(CH_3CN)_{10}$][OTf]$_4$ (**4c**). The isolation of **5** and **6** is in sharp contrast to our earlier observation of trans isomers of [$Re_2(L3)_2(CH_3CN)_4$][BF_4]$_4$ (L3 = NP-py and NP-tz) obtained from the reaction of [$Re_2(CH_3CN)_{10}$][BF_4]$_4$ with the corresponding ligands.[21] The only discernible difference is the degree of metal−metal bonding in $[Re_2]^{4+}$ and $[Mo_2]^{4+}$ precursors, the metal−metal bond order being three and four, respectively.

The addition of 2 equiv of [n-Bu_4N][OAc] to *cis*-[Mo_2(NP-tz)$_2(CH_3CN)_4$][BF_4]$_4$ provides the bis acetate compound **1**. Likewise, the addition of acetate ligands to *cis*-[Mo_2(NP-fu)$_2(CH_3CN)_4$][BF_4]$_4$ results in the trans isomer **2**. It should be noted at this point that the cis isomer of [$Mo_2(L3)_2(OAc)_2$]$^{2+}$ is formed when L3 is NP-tz, whereas a trans configuration of ligands is preferred for NP-fu regardless of the identity of the precursor molecules. Interestingly, only cis isomers are observed when the ancillary ligands are acetonitrile. Stepwise addition of acetates to *cis*-[Mo_2(NP-tz)$_2(CH_3CN)_4$][BF_4]$_4$ leads to **1** through the intermediacy of compound **7** which contains one acetate and two acetonitriles. Crystals of **7** were isolated in high yield (∼ 65%) by layering benzene onto acetonitrile solution of the bulk product. X-ray data reveal trans isomer in the solid state.

Solid-State Structures. The molecular structures of the dicationic units in **1**−**3** consist of a dimolybdenum unit spanned by two NP-R based ligands and two bridging

(20) Cotton, F. A.; Liu, C. Y.; Murillo, C. A. *Inorg. Chem.* **2004**, *43*, 2267.

(21) Bera, J. K.; Schelter, E. J.; Patra, S. K.; Basca, J.; Dunbar, K. R. *Dalton Trans.* **2006**, *33*, 4011.

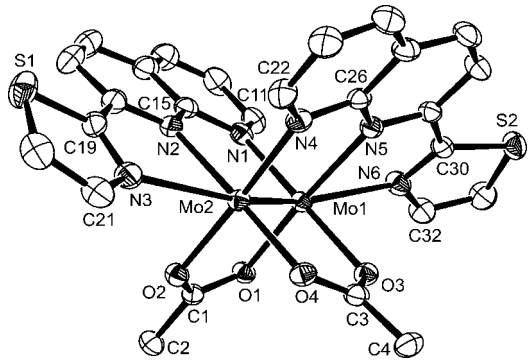

Figure 1. ORTEP diagram of the cationic unit *cis*-$[Mo_2(NP\text{-}tz)_2(OAc)_2]^{2+}$ in compound **1** with important atoms labeled. Hydrogen atoms are omitted for the sake of clarity. Thermal ellipsoids are drawn at the 50% probability level.

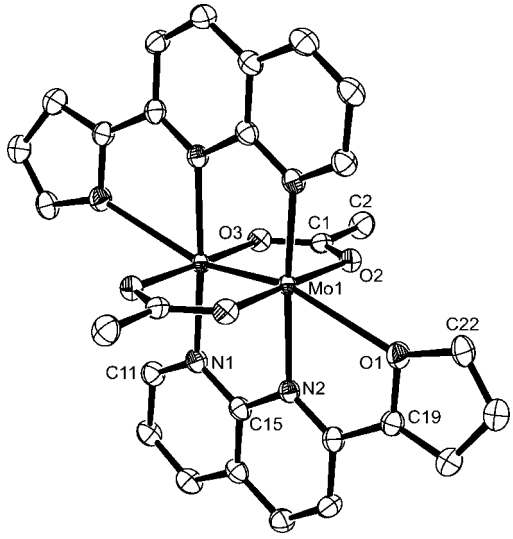

Figure 2. ORTEP diagram of the cationic unit *trans*-$[Mo_2(NP\text{-}fu)_2(OAc)_2]^{2+}$ in compound **2** with important atoms labeled. Hydrogen atoms are omitted for the sake of clarity. Thermal ellipsoids are drawn at the 50% probability level.

acetates as depicted in Figures 1−3. The N−C−N unit of the NP fragment bridges two molybdenum centers and the site trans to Mo−Mo quadruple bond is occupied by the donor atoms of the appendage at the 2-position. Thus two tridentate ligands occupy four equatorial and two axial sites of the dimolybdenum unit. The remaining four sites of the paddlewheel arrangement are occupied by bridging acetates. X-ray structures reveal that the NP-tz ligands in compound **1** are in a cis orientation (Figure 1). On the contrary, in compounds **2** and **3**, the NP-fu and NP-th ligands respectively are trans to each other (Figures 2 and 3). The molecular structure of **4**, as depicted in Figure 4, consists of two bidentate bridging NP-Me_2 ligands and two acetate groups. The disposition of the ligands is trans, akin to compounds **2** and **3**. Notably, the trans NP-Me_2 ligands are arranged in a head-to-head (HH) fashion (Figure 4). One of the axial sites of dimolybdenum unit is occupied by coordinated BF_4^- with a Mo-F distance of 2.496(1) Å, whereas the second axial site remains vacant. Weak interactions between the H_a protons (H11 and H21) and the F11 (2.437 and 2.396 Å, respectively) were observed. Presumably, the methyl substituents of NP-Me_2 ligands do not allow for the approach of ligands for axial coordination.

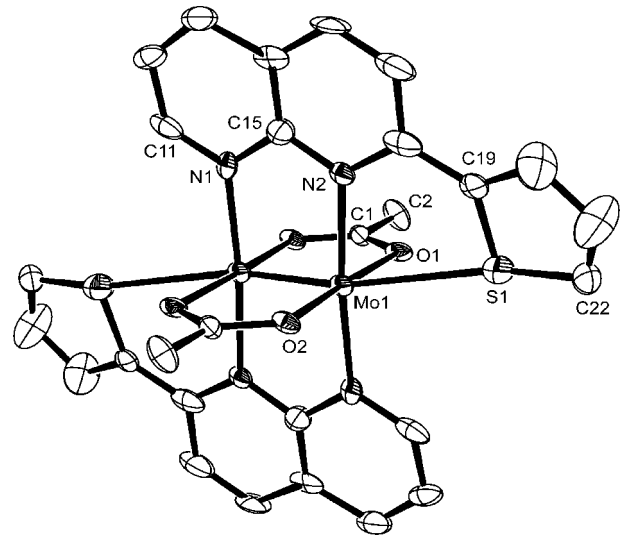

Figure 3. ORTEP diagram of the cationic unit *trans*-$[Mo_2(NP\text{-}th)_2(OAc)_2]^{2+}$ in compound **3** with important atoms labeled. Hydrogen atoms are omitted for the sake of clarity. Thermal ellipsoids are drawn at the 50% probability level.

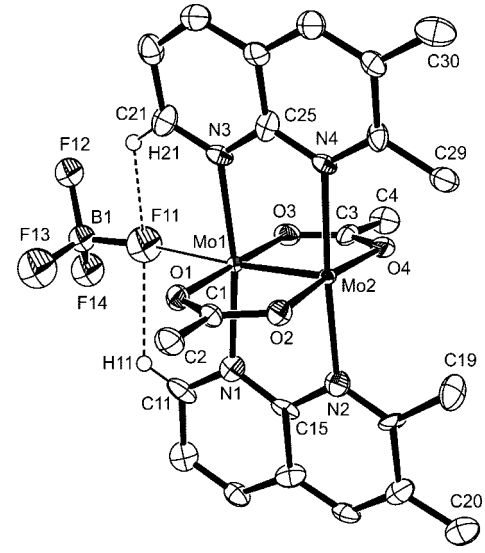

Figure 4. ORTEP diagram of the cationic unit *trans*-$[Mo_2(NP\text{-}Me_2)_2(OAc)_2][BF_4]^+$ in compound **4** with important atoms labeled. Hydrogen atoms except for H11 and H21 protons are omitted for the sake of clarity. Thermal ellipsoids are drawn at the 50% probability level.

The molecular structure of the tetracationic species $[Mo_2(NP\text{-}tz)_2(CH_3CN)_4]^{4+}$ in compound **5** consists of two cis NP-tz ligands spanning the dimolybdenum unit as in **1**. Each molybdenum center is additionally coordinated to two acetonitrile ligands (Figure 5).

The basic structure of **6**, shown in Figure 6, is essentially the same as that of **5** with the exception that the bridging ligands are NP-fu. An ORTEP plot of the *trans*-$[Mo_2(NP\text{-}tz)_2(OAc)(CH_3CN)_2][BF_4]_3$ (**7**) is shown in Figure 7. The tricationic unit in compound **7** is composed of two NP-tz ligands spanning the dimolybdenum unit, one bridging acetate and one acetonitrile molecule coordinated to each molybdenum atom. The X-ray structure of the compound reveals that the NP-tz ligands are oriented in a trans fashion.

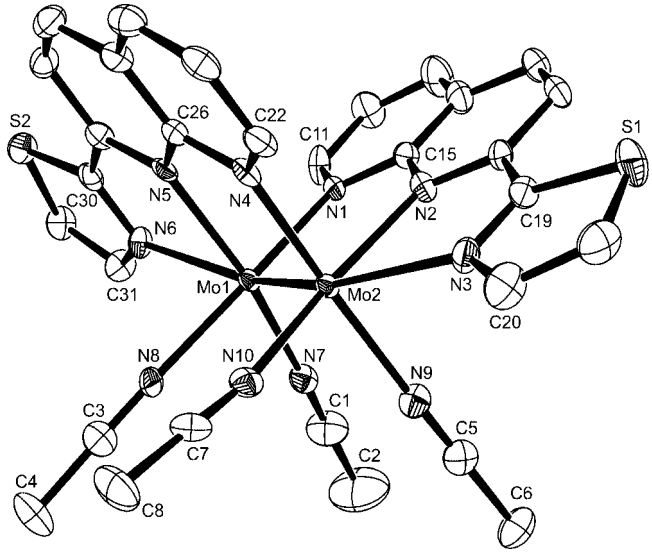

Figure 5. ORTEP diagram of the cationic unit *cis*-$[Mo_2(NP\text{-}tz)_2(CH_3CN)_4]^{4+}$ in compound **5** with important atoms labeled. Hydrogen atoms are omitted for the sake of clarity. Thermal ellipsoids are drawn at the 50% probability level.

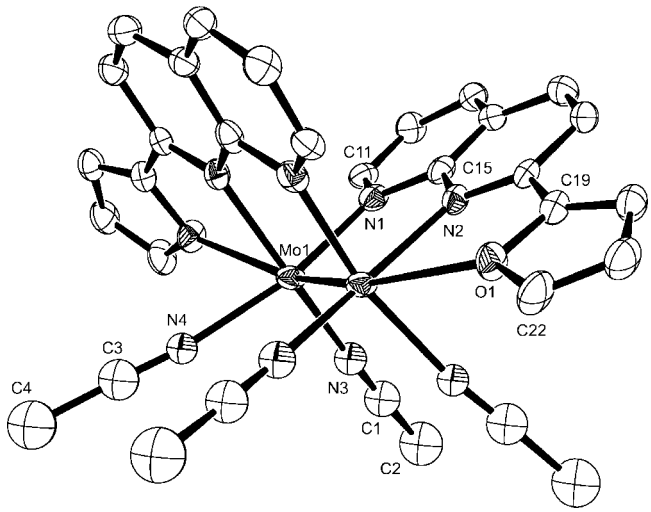

Figure 6. ORTEP diagram of the cationic unit *cis*-$[Mo_2(NP\text{-}fu)_2(CH_3CN)_4]^{4+}$ in compound **6** with important atoms labeled. Hydrogen atoms are omitted for the sake of clarity. Thermal ellipsoids are drawn at the 50% probability level.

The relevant bond distances and angles of compounds **1**−**7** are presented in Table 2. The Mo−Mo distance in the NP-tz complex **1** is 2.115(1) Å, similar to the value (2.124(1) Å) reported in the analogous compound *cis*-$[Mo_2(NP\text{-}py)_2(OAc)_2][BF_4]_2$.[7] The Mo-Mo distances in compounds **2** and **3** are shorter (2.087(1) and 2.078(3) Å). The metal-metal distances are the direct consequence of the interaction of different axial donors with the dimolybdenum unit.[22] The stronger pyridyl/thiazolyl donors destabilize the Mo-Mo σ-bond to a greater extent as compared to the furyl/thienyl donors leading to different metal-metal distances.[5] (c) The Mo−Mo distance in compound **4** is 2.081(1) Å, the compound that contains a weakly coordinated axial tetrafluoroborate anion.

The quadruply bonded Mo−Mo distances are also dependent on the number of bridging ligands. A significant lengthening of the Mo-Mo distance is noted when the

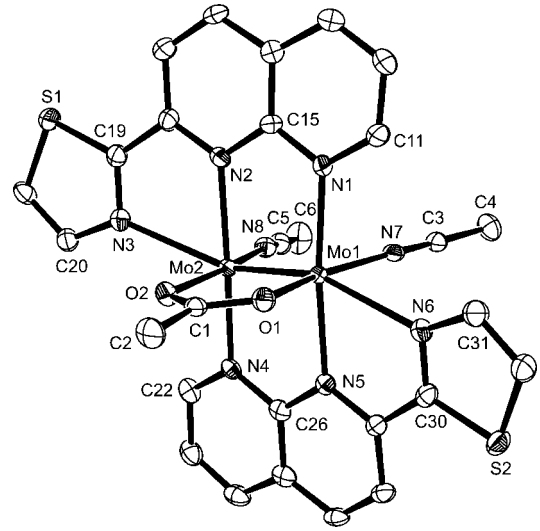

Figure 7. ORTEP diagram of the cationic unit *trans*-$[Mo_2(NP\text{-}tz)_2(OAc)(CH_3CN)_2]^{3+}$ in compound **7** with important atoms labeled. Hydrogen atoms are omitted for the sake of clarity. Thermal ellipsoids are drawn at the 50% probability level.

bridging acetate ligands in **1** (2.115(1) Å) are replaced by acetontrile in **5** (2.168(1) Å). Similarly, a small increase of 0.034 Å in the Mo−Mo distance is noted when two bridging acetates in **2** are replaced by acetonitrile molecules in **6**. It should be noted that the conversion of **2** to **6** proceeds with change in the orientation of the ligands from trans to cis. Compound **7** contains one bridging acetate and two acetonitriles, and the observed Mo−Mo distance of 2.147(1) Å is of intermediate length between **1** (which has two bridging acetate ligands) and **5** (with four acetonitrile groups).

Electrochemistry and Electronic Spectroscopy. Electrochemical studies of compounds **1**−**7** were performed in acetonitrile solution and their redox potentials are given in Table 3. Cyclic voltammogram of all complexes exhibit an irreversible metal-based oxidation peak and multiple ligand-centered reduction peaks.[23] Complex **1** exhibits four reversible reduction couples located at $E_{1/2}(1) = -0.35$ (65) V, $E_{1/2}$ (2) $= -0.53$ (65) V, $E_{1/2}$ (3) $= -1.21$ (76) V, and $E_{1/2}$ (4) $= -1.46$ (68) V. The CV features of **1** is identical to the NP-py analog $[Mo_2(NP\text{-}py)_2(OAc)_2][BF_4]_2$ reported earlier.[7] The irreversible metal-based oxidation occurs at $E_{p,a} = 1.06$ V. Similar electrochemical behavior were observed for **5** with reduction potentials located at $E_{1/2}$ (1) $= -0.03$ (64) V, $E_{1/2}$ (2) $= -0.29$ (65) V, $E_{1/2}$ (3) $= -0.98$ (69) V, and $E_{1/2}$ (4) $= -1.32$ (68) V. The free NP-tz exhibits two $1e^-$ reductions: the first reduction is reversible at potential $E_{1/2} = -1.49$ (87)

(22) (a) Bradley, P. M.; Bursten, B. E.; Turro, C. *Inorg. Chem.* **2001**, *40*, 1376. (b) Cotton, F. A.; Dikarev, E. V.; Petrukhina, M. A.; Stiriba, S-E. *Inorg. Chem.* **2000**, *39*, 1748. (c) Cotton, F. A.; Daniels, L. M.; Murillo, C. A.; Pascual, I.; Zhou, H. C. *J. Am. Chem. Soc.* **1999**, *121*, 6856. (d) Aullón, G.; Alvarez, S. *Inorg. Chem.* **1993**, *32*, 3712. (e) Clark, R. J. H.; Hempleman, A. J. *Inorg. Chem.* **1989**, *28*, 746. (f) Sowa, T.; Kawamura, T.; Shida, T.; Yonezawa, T. *Inorg. Chem.* **1983**, *22*, 56. (g) Nakatsuji, H.; Ushio, J.; Kanda, K.; Onishi, Y.; Kawamura, T.; Yonezawa, T. *Chem. Phys. Lett.* **1981**, *79*, 299. (h) Cotton, F. A.; Felthouse, T. R. *Inorg. Chem.* **1981**, *20*, 584. (i) Bursten, B. E.; Cotton, F. A. *Inorg. Chem.* **1981**, *20*, 3042. (j) Norman, J. G.; Kolari, H. J. *J. Am. Chem. Soc.* **1978**, *100*, 791. (k) Cotton, F. A.; Extine, M. W.; Rice, G. W. *Inorg. Chem.* **1978**, *17*, 176. (l) Dubicki, L.; Martin, R. L. *Inorg. Chem.* **1970**, *9*, 673.

Table 2. Comparison of Relevant Metrical Parameters for Compounds **1**−**7**

	1·0.5 CH_3CN	**2**	**3**·2CH_3CN	**4**
		bond lengths (Å)		
Mo−Mo	2.1151(7)	2.0866(8)	2.078(3)	2.0808(9)
Mo−X(ax)	2.526(4)	2.675(3)	2.942(5)	
	2.579(1)			
Mo−N(eq)	2.170(4)	2.216(3)	2.139(11)	2.213(7)
	2.251(3)	2.163(3)	2.203(11)	2.172(8)
	2.224(3)			2.232(7)
	2.178(4)			2.188(8)
Mo−O	2.096(3)	2.092(3)	2.084(8)	2.100(6)
	2.097(3)	2.092(3)	2.082(7)	2.127(7)
	2.107(3)			2.102(7)
	2.103(3)			2.087(7)
		bond angles (deg)		
Mo−Mo−X(ax)	158.72(9)	160.84(7)	167.42(12)	
	159.80(9)			
N(eq)−Mo−N(eq)	96.87(12)	173.43(12)	174.5(4)	171.0(3)
	92.79(12)			175.8(3)
N(eq)−Mo−X(ax)	69.96(13)	67.44(11)	75.1(3)	
	69.37(13)			
O−Mo−O	91.09(11)	176.23(11)	176.1(4)	178.9(3)
	91.95(11)			172.8(2)
		torsional angles (deg)		
N(eq)−C−C−X(ax)	7.54(10)	−0.52(5)	13.03(15)	
	−9.42(10)			
	5	**6**	**7**•C_6H_6	
		bond lengths (Å)		
Mo−Mo	2.1681(9)	2.1214(14)	2.1465(5)	
Mo−X(ax)	2.471(7)	2.633(6)	2.533(3)	
	2.515(7)		2.544(3)	
Mo−N(eq)	2.156(7)	2.137(8)	2.158(3)	
	2.205(7)	2.170(7)	2.227(3)	
	2.214(7)		2.248(3)	
	2.154(7)		2.163(3)	
Mo−O			2.072(3)	
			2.084(3)	
Mo−$NCCH_3$	2.138(8)	2.172(12)	2.154(3)	
	2.152(7)	2.172(11)	2.152(3)	
	2.164(7)			
	2.136(7)			
		bond angles (deg)		
Mo−Mo−X(ax)	160.80(17)	162.29(16)	159.12(8)	
	160.06(18)		157.40(8)	
N(eq)−Mo−N(eq)	92.7(2)	89.7(3)	174.27(12)	
	93.5(3)		175.23(12)	
N(eq)−Mo−X(ax)	71.1(2)	69.1(2)	70.05(12)	
	70.4(3)		69.31(12)	
CH_3CN−Mo−$NCCH_3$	85.1(3)	100.5(8)		
	90.4(3)			
		torsional angles (deg)		
N(eq)−C−C−X(ax)	−1.66(18)	−8.64(8)	−0.38(5)	
	0.88(18)		−1.34(5)	

Table 3. Electrochemical Potentials from Cyclic Voltammetry for Complexes **1**–**7**

compd	oxidation	reduction			
1	1.06[a]	−0.35 (65)[c]	−0.53 (65)[c]	−1.21 (76)[c]	−1.46 (68)[c]
2	1.33[a]	−0.47 (63)[c]	−0.64 (72)[c]		
3	1.26[a]	−0.59[b]	−0.71[b]		
4	1.20[a]	−0.82[b]	−1.04[b]		
5	1.60[a]	−0.03 (64)[c]	−0.29 (65)[c]	−0.98 (69)[c]	−1.32 (68)[c]
6	1.46[a]	−0.40 (71)[c]	−0.66 (72)[c]	−1.49[b]	
7	1.08[a]	−0.38[b]	−0.61[b]	−1.24[b]	−1.46[b]

[a] Peak potentials, $E_{p,a}$, for irreversible processes. [b] Peak potentials, $E_{p,c}$, for irreversible processes. [c] Half-wave potentials evaluated from cyclic voltammetry as $E_{1/2} = (E_{p,a} + E_{p,c})/2$, peak potential differences in mV in parentheses.

V and the second reduction is irreversible at $E_{p,c} = -2.16$ V. Two NP-tz ligands coordinated to quadruply bonded dimolybdenum(II) core result four 1e$^-$ reversible reductions indicative of electron delocalization in the mixed-valent intermediates.[5c] (c) For compound **1**, the separation between the first two reduction peaks is 186 mV, corresponding to the comproportionation constant $K_c(a) = 1.41 \times 10^3$. The separation between the third and fourth reversible reduction potential is 255 mV, larger than the difference between the first and second reduction processes. The corresponding $K_c(b)$ is 2.04×10^4. Both equilibrium constants indicate Class II weakly coupled systems in Robin-Day classification.[24] The

(23) (a) Marcaccio, M.; Paolucci, F.; Paradisi, C.; Roffia, S.; Fontanesi, C.; Yellowlees, L. J.; Serroni, S.; Campagna, S.; Denti, G.; Balzani, V. *J. Am. Chem. Soc.* **1999**, *121*, 10081. (b) Krejcik, M.; Vlcek, A. A. *Inorg. Chem.* **1992**, *31*, 2390. (c) Ohsawa, Y.; DeArmond, M. K.; Hanck, K. W.; Morris, D. E. *J. Am. Chem. Soc.* **1983**, *105*, 6522.

(24) (a) Robin, M. B.; Day, P. *Adv. Inorg. Chem. Radiochem.* **1967**, *10*, 247. (b) Kaim, W.; Klein, A.; Glöckle, M. *Acc. Chem. Res.* **2000**, *33*, 755.

Table 4. ^{1}H NMR Data (400 MHz, CD_3CN) for the NP-R Fragments in Corresponding Dimolybdenum (II) Compounds

	chemical shift, δ								
compds	H_a	H_b	H_c	H_d	H_e	H_f	H_g	H_h	-CH_3
1	7.83	7.78	8.81	8.98	8.57	8.01	7.48		2.67[a]
2	8.96	8.53	8.96	8.46	7.86	7.49	8.10	6.84	2.53[a]
4	8.88	8.05	8.88	8.73	2.57[b]	1.79[b]			2.59[a]
5	7.73	7.93	9.06	9.23	8.69	8.06	7.38		2.13[c]
6	7.97	8.97	9.01	8.47	7.92	7.39	7.83	6.87	2.13[c]
7	8.74	8.31	9.23	9.31	8.79	8.01	7.49		2.50[a], 2.13[c]

[a] Methyl (acetate). [b] Methyl (NP). [c] Methyl (acetonitrile).

estimated K_c(a) and K_c(b) values of complex **5** are 3.21×10^4, 5.9×10^5, indicating similar electrochemical behavior although the extent of electron delocalization is superior than that observed in **1**.

The free NP-fu and NP-th ligands exhibit reductions at −1.71 and −1.69 V, respectively. Complex **2** exhibits two reversible reduction waves at $E_{1/2} = -0.47$ (63) V and −0.64 (72) V. Irreversible reduction waves at $E_{p,c} = -0.59$ and −0.71 V were measured for **3**. The difference between the first and second reduction waves of compound **2** is 170 mV corresponding to $K_c(a) = 7.47 \times 10^2$ indicating poor electron delocalization in the reduced species. Substitution of acetates in **2** by acetonitriles leads to **6**, which exhibits reduction two reversible reduction potentials at $E_{1/2}$ (1) = −0.40 (71) V and $E_{1/2}$ (2) = −0.66 (72) V and an irreversible reduction wave at −1.49 V. The $K_c(a) = 2.39 \times 10^4$, obtained from the difference between the first and second reductions, is substantially higher than the corresponding value in **2**. Complex **4** displays reduction waves at $E_{p,c} = -0.82$ and −1.04 V and an irreversible metal-based oxidation occurs at $E_{p,a}$ =1.20 V. Multiple quasireversible reduction waves at −0.45, −0.64, −1.36, and −1.48 V are observed for complex **7**.

The electronic spectra of compounds **1**−**7** were recorded in acetonitrile in the range of 200–900 nm. The λ_{max} values with the corresponding ϵ values are given in the Supporting Information (Table S9). The spectra for all seven compounds display two sets of absorption bands in the visible region. The electron configuration of the paddlewheel $[Mo_2]^{2+}$ core is described as $\sigma^2\pi^4\delta^2$ and the likely assignment of the lowest energy electronic transition is the $\delta \rightarrow \delta^*$.[25] The electronic transitions in the range of 300–450 nm arise because of the $\delta \rightarrow d\pi^*$ transition.[26,27] The involvement of greater ligand character in the frontier orbitals results in large magnitude of their extinction coefficient.[5c,7]

^{1}H NMR Spectroscopy. The ^{1}H NMR spectra of **1**−**7** provide valuable insight into solution structure. The chemical shift values of protons for the compounds are listed in Table 4. Compound **1** exhibits seven nonequivalent aromatic protons, all of which have been assigned with reasonable certainty.[28] The data indicate an equivalence of the two NP-tz ligands on the NMR time scale. The chemical shift values

Scheme 5

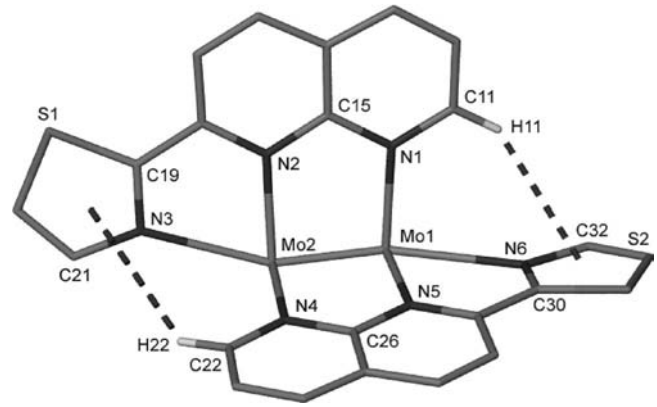

of four aromatic protons b−e (Scheme 1) appear downfield with respect to the free NP-tz (Table 4). Although downfield shifts of protons are expected because of coordination, the observed shifts of 0.28–0.93 ppm with respect to the free ligand appear to be rather large. However, the H_f of the thiazolyl appendage experiences an upfield shift of 0.45 ppm. The observed shift is attributed to the diamagnetic anisotropy of the Mo−Mo quadruple bond.[29] In a multiply bonded paddlewheel compound, protons residing in the equatorial region are observed downfield and those near in the axial region are observed upfield from their free form in the NMR spectra (see the Supporting Information, Scheme S2).[25] This fact explains the observed upfield shift of the H_f and downfield shifts of H_b−H_e protons. The H_g proton exhibits a marginal upfield shift of 0.06 ppm.

The most unusual signal is noticed for H_a, which is shifted upfield by 1.28 ppm. Such a large shift cannot be attributed solely to the diamagnetic anisotropic field around the Mo−Mo quadruple bond. A close inspection of the solid-state structure of **1** reveals that H_a protons of NP cores are positioned above the thiazolyl rings of the second NP-tz with H_a-X distances 3.110 and 3.633 Å, where X is the centroid of the thiazolyl ring (Scheme 5). The shielding caused by the appendage ring current[28,30] and Mo−Mo quadruple bond electrons result in large upfield shifts of the H_a protons.

The six proton signals corresponding to two methyl groups of the bridging acetates appear as a sharp singlet at 2.67 ppm indicative of a single cis compound in solution in NMR time scale.

The ^{1}H NMR spectrum of **2** reveals eight distinct aromatic protons. The H_a and H_f protons (Scheme 1) are shifted upfield ($\Delta\delta$ = 0.08 ppm, 0.61 ppm), as they are aligned along the M−M quadruple bond and lies in the shielding zone. The remaining protons are shifted downfield ($\Delta\delta$ = 0.38–0.90) as expected. The normal upfield shift of H_a, $\Delta\delta$ = 0.08 ppm indicates a trans arrangement of NP-fu ligands which does not allow the ring current of the furyl to affect H_a. Thus the magnitude of upfield chemical shift difference of H_a proton

(25) Cotton, F. A.; Murillo, C. A.; Walton. R. A. *Multiple Bonds Between Metal Atoms*, 3rd ed.; Springer Science and Business Media: New York, 2005.
(26) Trogler, W. C.; Gray, H. B. *Acc. Chem. Res.* **1978**, *11*, 232.
(27) Trogler, W. C.; Solomon, E. I.; Trajberg, I. B.; Ballhausen, C. J.; Gray, H. B. *Inorg. Chem.* **1977**, *16*, 828.
(28) Tikkanen, W.; Binamira-Soriaga, E.; Kaska, W.; Ford, P. *Inorg. Chem.* **1984**, *23*, 141.
(29) Cotton, F. A.; Daniels, L. M.; Lei, P.; Murillo, C. A.; Wang, X. *Inorg. Chem.* **2001**, *40*, 2778.
(30) Thummel, R. P.; Lefoulon, F.; Williamson, D.; Chavan, M. *Inorg. Chem.* **1986**, *25*, 1675.

with respect to the free ligand is diagnostic of the cis/trans disposition of ligands. The two acetates protons appear at 2.53 ppm. A careful inspection of the NMR spectrum of **2** reveals additional signals in the aromatic regions. The methyl region also shows two additional low intensity signals assigned as acetate protons at 2.67 and 2.59 ppm. This set of signals is attributed to a product arising from asymmetrically bridged acetate ligands in solution (vide infra).

The axial proton H_f and H_g in **5** and **6** are shifted upfield (0.75 – 0.15 ppm) and equatorial protons are shifted downfield in accordance with the earlier described observations. The H_a protons exhibit upfield shifts of 1.37 ppm and 1.08 ppm indicative of a cis arrangement of NP-tz and NP-fu ligands in compounds **5** and **6** respectively. In both cases, a sharp methyl signal appears that corresponds to the acetonitrile ligands.

All seven proton signals in ^{1}H NMR spectrum of **4** are accounted for its trans geometry. As in the previous cases, the b−d protons, as well the methyl protons (H_e), are deshielded (Scheme 1). The ortho methyl protons (marked as H_f) lying in the shielding zone of the M−M bond are shifted upfield by 0.93 ppm with respect to the free ligand. The H_a protons of two NP ligands are shifted upfield, by 0.07 ppm, remarkably similar to that observed for **2**. The trans isomers **2** and **4** exhibit a low magnitude for $\Delta\delta$ shifts of their H_a protons. The six methyl protons of the bridging acetate ligands appear as a sharp singlet at 2.59 ppm, indicating a single species is present in solution on the NMR time scale.

The spectral data confirms that cis structures of **1**, **5**, and **6** and trans structures of **2** and **4**, as determined from X-ray studies in the solid state, are retained in solution. The value of chemical shift difference $\Delta\delta$ of Ha protons around 0.1 ppm is characteristic for trans geometry, whereas the corresponding values that are greater than 1 ppm signify a cis orientation of the ligands.

Single crystals of *trans*-$[Mo_2(NP\text{-}tz)_2(OAc)(CH_3CN)_2][BF_4]_3$ (**7**) were used for NMR experiments. The bulk product did not exhibit discernible ^{1}H NMR features. The ^{1}H NMR spectrum of the trans product **7** exhibits 13 nonequivalent proton resonances indicating that two distinct products exist in CD_3CN. A careful examination of the data reveals a mixture of cis and trans isomers for **7** in a ratio of 1:1.3, a fact that clearly indicates geometry conversion in solution. The methyl protons of the single bridging acetate ligand in these two isomers appear at 2.43 and 2.50 ppm. All aromatic protons were assigned for the two isomers, with two of them being overlapping signals. The resonances appearing at 7.97 and 8.74 ppm are assigned to H_a protons. The signal at 7.97 ppm with a chemical shift difference $\Delta\delta$ of 1.13 ppm is ascribed to the cis isomer, whereas the 0.36 chemical shift difference of the signal at 8.74 ppm is attributed to the presence of the trans isomer of **7**. Given the fact that the bis-acetate product **1** and the tetraacetonitrile complex **5** exist as cis isomers, it is not surprising that the monoacetate species, **7**, results in the mixture of cis as well as the trans structure in solution.

Cis/Trans Isomerization. The cis/trans disposition of ligands in "$Mo_2(OAc)_2(L)_2$" has been addressed by several groups.[31] The structure of a given product is rationalized on the basis of the interplay of kinetic and thermodynamic stabilities.[20] It is, therefore, informative to discuss the order of basicity and lability of the ligands as they pertain to the cis/trans isomerization processes. In previous work, Cotton and Murillo rationalized the substitution reactions in dimolybdenum(II)-formamidinate compounds on the basis of ligand labilities.[20] A similar line of reasoning is invoked for naphthyridine analogs. Acetonitrile ligands are easily replaced by acetates and NP-R ligands. Although the acetate groups are replaced by NP-R ligands in the presence of suitable anions, the reverse reactions are not observed under the reaction conditions studied. Acetate ligands are readily substituted by acetonitrile, but only in the presence of $HBF_4 \cdot Et_2O$ or Et_3OBF_4, which serve to protonate and alkylate the carboxylate group, respectively. The reaction patterns reflect the basicity of the three ligands in the order NP-R > acetate > acetonitrile. The lability is the opposite, with the NP-R ligand being the most difficult to displace and the acetonitrile ligand being the most easily substituted. The trans effect exerted by these ligands is proportional to their basicity.

As the results of this study revealed, a given precursor molecule does not necessarily lead to a product with retention of the initial geometry. The configurations of the compounds isolated in this work are rationalized based on the trans effect of the ligands and the thermodynamic stability of the products. The six acetonitrile ligands in *cis*-$[Mo_2(OAc)_2(CH_3CN)_6]^{2+}$ are replaced by NP-py or NP-tz with retention of geometry as observed in *cis*-$[Mo_2(OAc)_2(NP\text{-}py)_2]^{2+}$ and **1**. Isolation of the cis isomers is not surprising, as they are thermodynamically more stable.

The use of NP-fu or NP-th results in the trans isomers **2** and **3** respectively. It appears that NP-R ligands that possess stronger axial donors such as pyridyl and thiazolyl in NP-py and NP-tz, respectively, lead to the cis isomers, whereas ligands with the weaker appendages (furyl and thienyl in NP-fu and NP-th) result in trans isomers. The isolation of the trans compounds **2**, **3**, and **4** suggests that geometry conversion takes place during replacement of acetonitriles by the ligands. Axial coordination of the acetate has been invoked in a stepwise isomerization process.[32] A possible sequence of steps in the substitution and isomerization

(31) (a) Yamaguchi, Y.; Ozaki, S.; Hinago, H.; Kobayashi, K.; Ito, T. *Inorg. Chim. Acta* **2005**, *358*, 2363. (b) Zou, G.; Ren, T. *Inorg. Chim. Acta* **2000**, *304*, 305. (c) Xue, W. M.; Kuhn, F. E.; Zhang, G.; Herdtweck, E.; Sieber, G. R. *J. Chem. Soc., Dalton Trans.* **1999**, 4103. (d) Tanase, T.; Igoshi, T.; Kobayashi, K.; Yamamoto, Y. *J. Chem. Res.* **1998**, 538. (e) Day, E. F.; Huffman, J. C.; Folting, K.; Christou, G. *J. Chem. Soc., Dalton Trans.* **1997**, 2837. (f) Acho, J. A.; Ren, T.; Yun, J. W.; Lippard, S. J. *Inorg. Chem.* **1995**, *34*, 5226. (g) Matonic, J. H.; Chen, S. J.; Perlepes, S. P.; Dunbar, K. R.; Christou, G. *J. Am. Chem. Soc.* **1991**, *113*, 8169. (h) Allaire, F.; Beauchamp, A. L. *Inorg. Chim. Acta* **1989**, *156*, 241. (i) Cotton, F. A.; Ilsley, W. H.; Kaim, W. *Inorg. Chem.* **1981**, *20*, 930.

(32) (a) Crawford, C. A.; Matonic, J.; Streib, W. E.; Huffman, J. C.; Dunbar, K. R.; Christou, G. *Inorg. Chem.* **1993**, *32*, 3125. (b) Cayton, R. H.; Chacon, S. T.; Chisholm, M. H.; Folting, K. *Polyhedron* **1993**, *12*, 415. (c) Chifotides, H. T.; Dunbar, K. R. *Acc. Chem. Res.* **2005**, *38*, 146. (d) Howell, J. A. S. *Dalton Trans.* **2007**, 3798.

Scheme 6

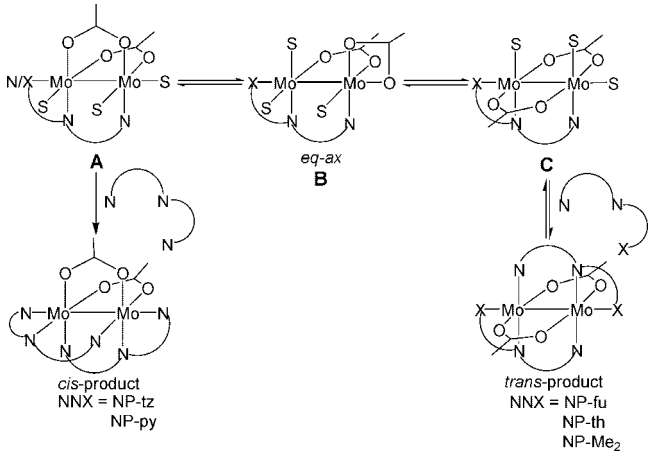

process is outlined in Scheme 6. In the stepwise transformation, the acetate group trans to the NP ligand in **A** is activated, which leads to the cleavage of one of the Mo−O bonds. Subsequently, the acetate ligand rearranges from a μ-bridging mode to a chelating eq−ax disposition of O-atoms as shown in **B**. Precedence for this step exists as discussed in several reports. A solution of $Mo_2(\mu\text{-}CO_2CF_3)_4$ in pyridine has been shown to contain $Mo_2(\mu\text{-}O_2CCF_3)_2(\eta^1\text{-}O_2CCF_3)_2(Py)_4$ in which there are two equatorial and two axial pyridine ligands, an indication of Mo−O bond cleavage.[33] In addition, intermediates involving eq−ax acetate ligands in dimetal chemistry have been isolated and structurally characterized.[32,34] In the next step, the acetate anion displaces the labile CH_3CN molecules thereby completing the geometry conversion (**C**). The second NNX replaces the acetonitrile ligands in the product formation step, leading to the trans derivatives **2**, **3**, and **4**.

It is apparent that the NP-py/NP-tz ligands bind faster with **A** relative to the acetate migration. For any ligands to enter or leave the M_2 coordination sphere, the axial sites are the most likely pathway.[35] The stronger pyridyl/thiazolyl donors replace the axial acetonitrile ligands in **A**, and subsequently the NP core displaces the equatorial acetonitrile ligands to bridge the dimolybdenum unit. The result is the formation of cis products. In the case of weak appendages such as furyl or thienyl, the acetate migration prevails over the axial coordination of NP-fu/NP-th, the result of which is conversion to the trans isomer.

The intermediacy of **B** involving both the eq−ax chelating acetate as well the μ-bridging was observed in the ^{1}H NMR spectrum of **2**. Two low-intensity acetate peaks in the ratio of 1:1 at 2.67 and 2.59 ppm are observed in addition to the distinct peak at 2.53 ppm, assigned for the bridging acetates in **2**. A group of weak signals was also observed in the aromatic region in accord with the existence of the intermediate **B**. No intermediate species was noted in the case of NP-py/NP-tz complexes, as confirmed from the singlet signals of the acetate protons in the ^{1}H NMR spectra.

In the case of complex **4**, the presence of two methyl groups at the 2-positions of the head-to-head NP ligands and an axially coordinated tetrafluoroborate anion results in a kinetically protected structure (Figure 4) which would be expected to hinder acetate migration once the product is formed. Indeed, the NMR spectrum reveals the presence of the pure trans isomer.

Controlled protonation of **2** with triflic acid in acetonitrile led to the replacement of the acetate ligands with acetonitrile groups to produce *cis*-$[Mo_2(NP\text{-}fu)_2(CH_3CN)_4][OTf]_4$ (**6**) as the thermodynamically stable product. The isomerization involved in the replacement of acetate by acetonitriles has been observed in the reaction of *trans*-$Mo_2(DAniF)_2(O_2CCH_3)_2$ with 2 equiv of triethyloxonium tetrafluoroborate to give *cis*-$[Mo_2(DAniF)_2(CH_3CN)_4]^{2+}$.[20] In the present case of **7**, however, the compound does not favor one geometry as being much more stable than the other. Although compound **7** was isolated as the trans isomer in crystals that were analyzed by X-ray methods, there is an equilibrium between the cis and trans isomers in solution as confirmed by ^{1}H NMR data.

Conclusions

It has been found that in the class of ligands used in this study, namely NP-R groups, the geometry of the dicationic moiety "$Mo_2(OAc)_2(NP\text{-}R)_2$" is mediated by the nature of the R group. The stronger pyridyl and thiazolyl donors result in cis isomers and the weaker bases furyl and thienyl lead to the trans orientation of the ligands. A bidentate NP ligand with no coordinating group at the 2-position led to a trans structure with an anion occupying one axial site. Only cis isomers are isolated, regardless of the identity of axial donors, when the ancillary ligands are acetonitrile. The combination of one acetate and two acetonitrile ligands leads to the trans structure in the solid state. The cis and trans isomers are distinguishable by their ^{1}H NMR spectra, which is convenient for probing the differences in solid-state versus solution structures. The isolation of trans compounds indicates that isomerization from cis to trans takes place during the reactions. An acetate migration through an intermediate axial coordination mode has been invoked to rationalize the trans products for ligands with weak axial donors and retention of cis configurations for strong axial donors.

Acknowledgment. We thank the reviewers for their valuable comments and insight. J.K.B. thanks the CSIR and DST India for support of this research. K.R.D. thanks the Robert A. Welch Foundation for generous support.

Supporting Information Available: X-ray crystallographic data for compounds **1**−**7**; synthetic procedures of the ligands, tables of bond distances and bond angles for the compounds, and NMR (PDF). This material is available free of charge via the Internet at http://pubs.acs.org.

IC702298V

(33) Webb, T. R.; Dong, T. Y. *Inorg. Chem.* **1982**, *21*, 114.
(34) Casas, J. M.; Cayton, R. H.; Chisholm, M. H. *Inorg. Chem.* **1991**, *30*, 358.
(35) Chifotides, H. T.; Catalan, K. V.; Dunbar, K. R. *Inorg. Chem.* **2003**, *42*, 8739.